J. Anat. (2001) **199**, pp. 567–576, with 12 figures Printed in the United Kingdom

The three-dimensional microanatomy of the rabbit and human cornea. A chemical and mechanical microdissection-SEM approach

JOSÉ L. OJEDA[1], JUAN A. VENTOSA[2] AND SONSOLES PIEDRA[1]

[1] *Department of Anatomy and Cell Biology*, *and* [2] *Ophthalmology Unit*, *University of Cantabria*, *Spain*

(*Accepted 25 June 2001*)

ABSTRACT

The three-dimensional (3D) microanatomy of the cornea is the major determinant of its optical and mechanical properties. Scanning electron microscopy (SEM) is the most commonly used method to obtain information on the overall 3D microanatomy of organs. However, SEM has not been successful in revealing the 3D microanatomy of the cornea, because the interior of the cornea is too compact to be explored by the electron beam. In this study, the 3D organisation of the cells and extracellular materials of human and rabbit corneas was examined after exposure by HCl and NaOH digestion, and by microdissection by the adhesive tape method. In the cornea of both species, all epithelial cells exhibited microplicae regardless of their location. This raises doubts about the tear film-holding role assigned to the microplicae of the superficial cells. Human and rabbit corneas differed in the collagen fibre patterns of the epithelial basement membranes. The 3D organisation of the stromal lamellae was similar in both species. In humans and rabbits, the keratocytes showed similar 3D features. However, the surface of human keratocytes located near Descemet's membrane exhibited small fenestrations that were not present in the rabbit keratocytes. The pattern of keratocyte innervation by the stromal neural plexus and 3D keratocyte microanatomy confirms that keratocytes form a large intercommunicating network within the corneal stroma. Two morphologically discrete subpopulations of keratocytes located at different stromal levels were identified in both human and rabbit corneas, suggesting that keratocytes are not functionally homogeneous. In addition, the density of the stromal neural plexus appeared to be greater in rabbits than in humans. Clear differences between human and rabbit corneas were observed in the collagen arrangement in Descemet's membrane, which may reflect their different biomechanical requirements.

Key words: Keratocytes; cornea; ultrastructure.

INTRODUCTION

Understanding the complexity of the microanatomy of the normal cornea requires the combined use of many strategies and methods. Scanning electron microscopy (SEM) is a versatile method, because it provides direct information on the overall three-dimensional (3D) organisation of the specimen examined.

Most SEM studies of the cornea have been restricted to the apical surfaces of the epithelium and the endothelium (see Doughty, 1990). Since the interior of the cornea is too compact to be explored by the electron beam, and its cellular components are completely embedded in extracellular matrices, SEM has not been successful in revealing the overall morphology of the cornea. However, knowledge of corneal microanatomy is essential for an understanding of its pathology because the 3D organisation of the extracellular matrix and cells is the major determinant of the optical and mechanical properties of the cornea (Klyce & Beuerman, 1988; Beuerman & Pedroza, 1996). The introduction of chemical microdissection methods (see Ojeda, 1997), which allow

Correspondence to Prof. José L. Ojeda, Departamento de Anatomía y Biologìa Celular, Facultad de Medicina, Cardenal Herrera Oria s/n, 39011 Santander, Spain. e-mail: ojedajl@unican.es

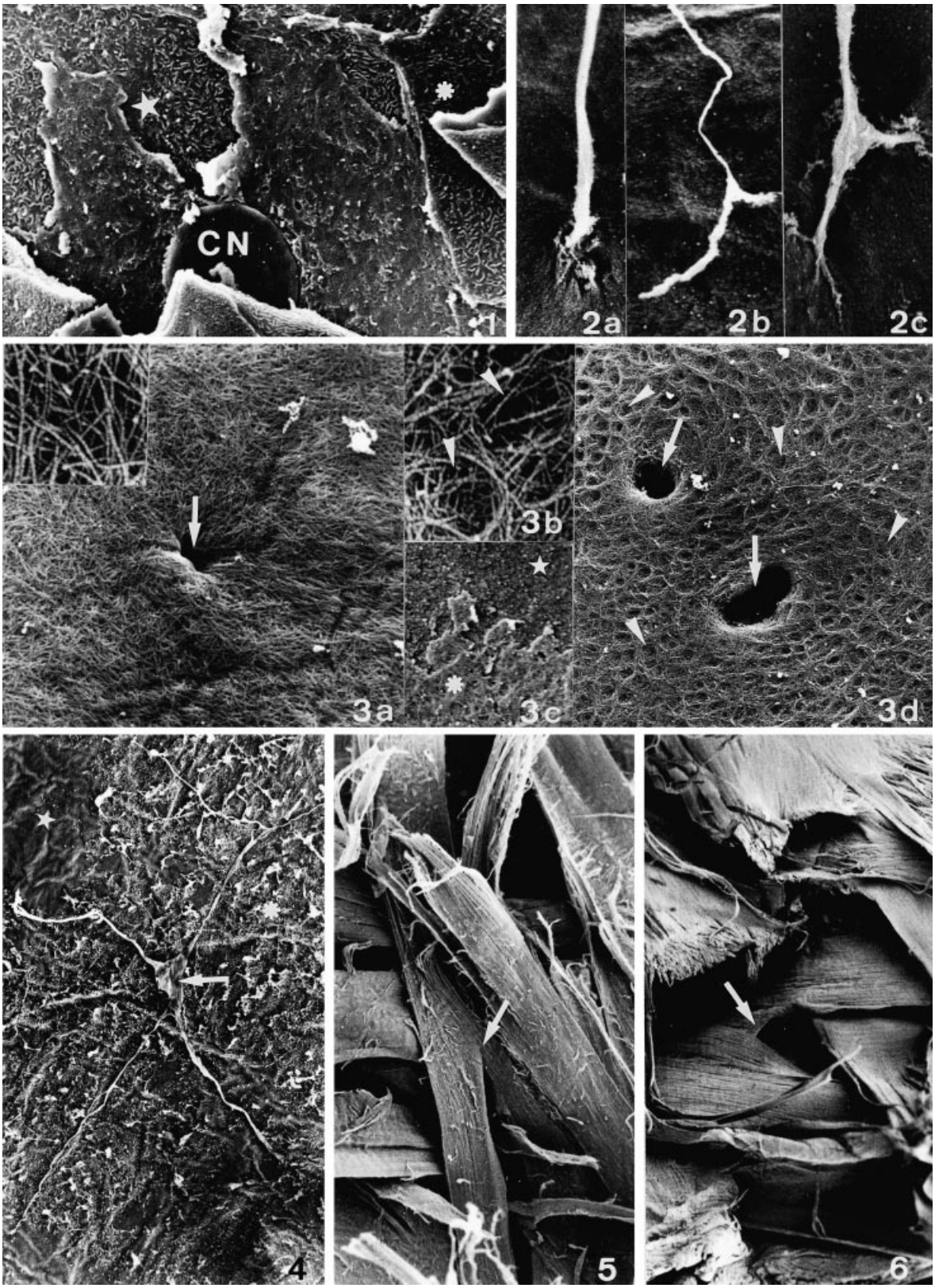

Fig. 1. Anterior view of the epithelium in a rabbit cornea microdissected by the adhesive tape method. Note that the cells of the second (asterisk) and third (star) epithelial layers exhibit numerous microplicae. CN, cell nucleus. $\times 2500$.

Fig. 2. Basal views of the epithelium of two rabbit (*a*, *c*) and one human (*b*) corneas exposed by HCl digestion which show penetration of nerve fibres. In (*a*) the fibre penetrates without division, whereas the fibres bifurcate in (*c*) and branch several times in (*b*) before penetration. $\times 2500$ (*a*, *c*); $\times 1250$ (*b*).

selective removal of the extracellular matrix or cell organ components, has greatly extended the application of SEM for study of the interior of compact organs. However, to date, these methods have not been used in a systematic 3D microanatomical study of the cornea.

The present paper describes new aspects of the 3D organisation of the cells and extracellular materials in human and rabbit corneas exposed by chemical and mechanical dissection. A comparative study of the cornea in humans and rabbits was undertaken because the rabbit is commonly used in corneal research.

MATERIALS AND METHODS

Rabbit and human corneas were used in this study. New Zealand white rabbits (n = 10) of both sexes and weighing 2–3 kg were used. Animals were euthanised by an injection of 100 mg/kg pentobarbital sodium into a peripheral ear vein. Immediately after death, several drops of cacodylate-buffered 2% paraformaldehyde and glutaraldehyde 0.5%, pH 7.3, were gently instilled onto the corneal surface. The contents of the anterior chamber were then replaced with fixative by means of a 27-gauge needle inserted close to the limbus after a puncture hole had been made close to the limbus on the other side of the limbus. After enucleation of the globe, the cornea was freed from the underlying tissues, transferred to a vial of fixative and placed in a refrigerator at 4 °C for 10 h.

Eight human autopsy eyes (4–10 h postmortem) were used. Proper informed consent was obtained in all cases. The donors were males and females between 18 and 41 y old, and there was no evidence that they suffered from ophthalmological disease. The specimens were fixed in the same fixative as the rabbit corneas.

After fixation, rabbit and human corneas were rinsed in the cacodylate buffer and subjected to chemical and mechanical microdissection. For chemical microdissection, 2 complementary procedures were used. To visualise cellular components, small corneal fragments were digested with HCl (Evan et al. 1976). Collagenase digestion was omitted in all cases. To visualise the extracellular material, small corneal fragments were digested with NaOH (Ohtani, 1987). After chemical digestion, some specimens were carefully microdissected under a stereo-microscope with sharpened tungsten needles. The specimens were dehydrated in graded acetone, dried by the critical point method, and attached to aluminium stubs with silver paint.

After drying, some specimens were dissected mechanically with the adhesive tape method (De Ruiter et al. 1993).

All specimens were coated with gold/palladium and viewed with a Philips SEM 501.

RESULTS

Epithelium

Microdissection with the adhesive tape method exposed the surface of the cells located in the deeper portion of the superficial or squamous cell layer. All cells in the deeper portions showed numerous microplicae, which were wider and more elaborate than those in the light superficial cells (Fig. 1). After removal of the extracellular material, the basal pole of the corneal epithelium appears as a smooth surface, on which the cell boundaries cannot be resolved (Fig. 2*a*, *b*). This surface was perforated randomly by numerous nerve fibres. In most cases, these fibres penetrate the epithelium without division (Fig. 2*a*). However, in some cases the fibres branched 2 or more times immediately before penetration (Fig. 2*b*, *c*).

The microanatomy of the corneal epithelium and its innervation showed no significant differences between rabbits and humans. In contrast, the epithelial basement membrane (EBM) was clearly different. The rabbit EBM appears as a flat network of straight fibres with no defined order (Fig. 3*a*, inset), whereas the human EBM exhibits a network of straight and curved fibres, forming characteristic birdnest-like structures (Fig. 3*b*, *d*).

Both the rabbit and the human EBM were formed by a thin layer of fibres (Fig. 3*c*) that showed periodic cross striations (Fig. 3*a* inset, 3*b*), and both EBMs

Fig. 3. Micrographs of the epithelial basement membrane anterior surface after removal of the corneal epithelium by NaOH digestion. Note that in the rabbit cornea (*a*, inset) the fibres run without a defined pattern, whereas in the human cornea (*b*, *c*, *d*) they form characteristic repeating patterns (arrowheads). In (*c*), the epithelial basement membrane (asterisk) was partially eliminated by adhesive tape dissection, showing it to consist of a thin layer of fibres in close relationship to the anterior face of Bowman layer (star). Arrows, holes. ×2500 (*a*, *c*, *d*); 13000 (inset *b*).

Fig. 4. Anterior view of the epithelial basement membrane (asterisk) of a partially HCl-digested, rabbit cornea showing the subepithelial plexus. Arrow, Schwann cell; star, epithelial basal surface. ×650.

Figs 5, 6. Micrographs showing the arrangement of lamellae within the rabbit (Fig. 5) and human (Fig. 6) corneal stroma. NaOH digestion. Arrows, bifurcation of lamellae. ×160.

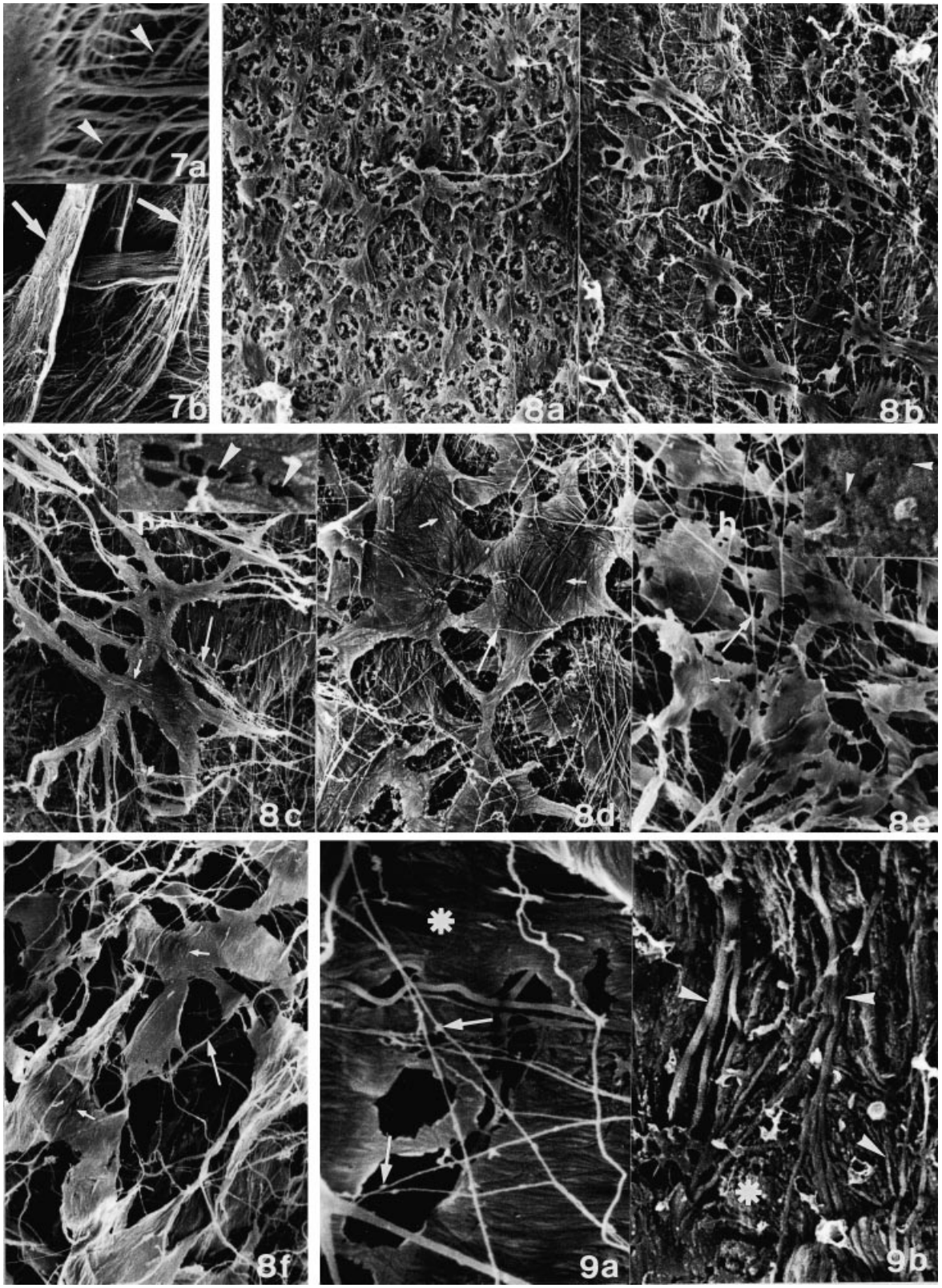

Fig. 7. Detailed views of lamellae demonstrating their collagen fibre arrangement. Arrowheads, collagen fibres arranged transversally. Arrows, collagen fibres running antero-posteriorly and joining two lamellar layers. NaOH digestion. (*a*) Human cornea; (*b*) rabbit cornea. ×10000 (*a*); ×2500 (*b*).

Fig. 8. Images of the network of keratocytes in the rabbit (*a–d*) and human (*e*, *f*) corneal stroma exposed by HCl digestion. (*a*, *d*, *f*) keratocytes in anterior stroma; (*b*, *c*, *e*) keratocytes in posterior stroma. Detailed views of large and medium-sized fenestrations (*c* inset, small arrowheads) and of a field of small fenestrations (*e* inset, small arrowheads). Short arrows, furrows; large arrows, stromal neural plexus. ×325 (*a*, *b*); ×1400 (*c*, *d*); ×1250 (*e*, *f*); ×6000 (insets).

presented numerous holes (Fig. 3 *a*, *d*), presumably occupied by the nerve fibres for the corneal epithelium.

Partial HCl digestion of the corneas allowed observation of the subepithelial plexus directly opposed to the EBM inner surface (Fig. 4). In both rabbit and human corneas, the plexus consisted of nerves that frequently bifurcated and anastomosed, thus forming a loose network. Occasionally the nerve fibres exhibited varicosities (Fig. 4).

Stroma

Chemical and mechanical microdissection of the cornea exposed the 3 basic components: lamellae, keratocytes and the stromal neural plexus.

In the rabbit and human cornea, the lamellae appear as flattened ribbons arranged in superposed layers parallel to the corneal surface (Fig. 5). Their thickness was uniform but their width was extremely variable (from 7 to 250 μm). This variation occurred not only between different lamellae, but also within the same lamella. The lamellae frequently branch out in 2 or 3 subsidiary branches (Figs 5, 6), sometimes remaining in the same layer and sometimes forming part of a contiguous layer (Fig. 6). Thus the lamellae of the corneal stroma were not merely superposed but formed a truly intertwined structure (Fig. 6). No differences in their morphology or in their arrangement were observed in relation to their position within the cornea.

Most of the collagen fibres constituting the lamellae were packed in parallel arrays that followed the lamellar long axis; however, some fibres lay almost transverse to this axis, and others ran perpendicular to the corneal surfaces to join two lamellae located in different layers (Fig. 7 *b*). After NaOH digestion, the lamellar collagen fibres appeared less compactly packed in the human than in the rabbit cornea.

Within the same stromal layer, the long axes of the lamellae were oriented in different directions. The lamellae located in contiguous layers were seen to cross each other at many different angles (Figs 5, 6), but only occasionally at right angles.

After removal of the stromal extracellular matrix by HCl digestion, the keratocytes were readily viewed by SEM. In humans and rabbits, they appeared as flattened cells, lying parallel to the corneal surface, and were stellate with several cellular processes (Fig. 8 *a*, *b*) that made contact with neighbouring keratocytes or less frequently with keratocyte bodies. By SEM, no discontinuities were observed in the area of contact between two keratocytes so that the keratocytes appeared layered and arranged like a syncytium (Fig. 8 *a*, *b*). Occasionally, keratocyte bodies and their processes were seen to be orientated obliquely, forming bridges from one keratocyte layer to the next.

The keratocyte surface was furrowed by numerous linear depressions (Fig. 8 *c–f*), lying parallel to one another and, after incomplete HCl digestion, collagen fibres were observed in association with these depressions. Unlike what tends to occur in other flat cells, the keratocyte surface did not exhibit nuclear bulges.

In the rabbit cornea, the keratocyte density (number of keratocytes per surface unit) differed according to the stromal level. In Figure 8 *a* and *b*, the keratocyte density is seen to be about 3 times higher in the anterior stroma (the half of the stroma nearer the epithelium) than in the posterior stroma. Morphologically, the keratocytes were a heterogeneous cell population in both rabbits and humans. In the rabbit, the keratocytes located in the posterior stroma (PSK) were characterised by the presence of long slender cellular processes that branched three to five times (Fig. 8 *c*) before making contact with other keratocytes. These keratocytes usually sent out cell processes from 2 opposite points of the keratocyte body so that they can be described as forming a rectangular outline. In addition, the PSK possessed large and medium-sized fenestrations (Fig. 8 *c*, inset). In contrast, the keratocytes of the anterior stroma (ASK) presented short wide cellular non-branching processes (Fig. 8 *d*) sent out radially from the keratocyte body (Fig. 8 *d*). Thus the ASK can be described as having a circular outline, and no fenestrations were observed in the ASK.

In the human cornea, the PSK cellular processes were, as in the rabbit, long and slender, but only occasionally branching (Fig. 8 *e*). The most characteristic feature of the PSK was the presence of numerous small fenestrations grouped in fields (Fig. 8 *e*, inset). Occasionally, some medium-sized fenestrations were present in the PSK. In contrast to what was seen in the rabbit cornea, the ASK cellular processes were not arranged radially and were extremely wide (Fig. 8 *f*), so that it was difficult to distinguish the cellular processes from the cell body.

The corneal stroma contained a network of axons

Fig. 9. Micrographs showing the keratocyte-stromal neural plexus relationships. Note (*a*) the varicosities (arrows) and (*b*) the great number of axons (arrowheads) in close contact with one keratocyte. Rabbit corneas. HCl digested. Asterisk, keratocyte. × 5000.

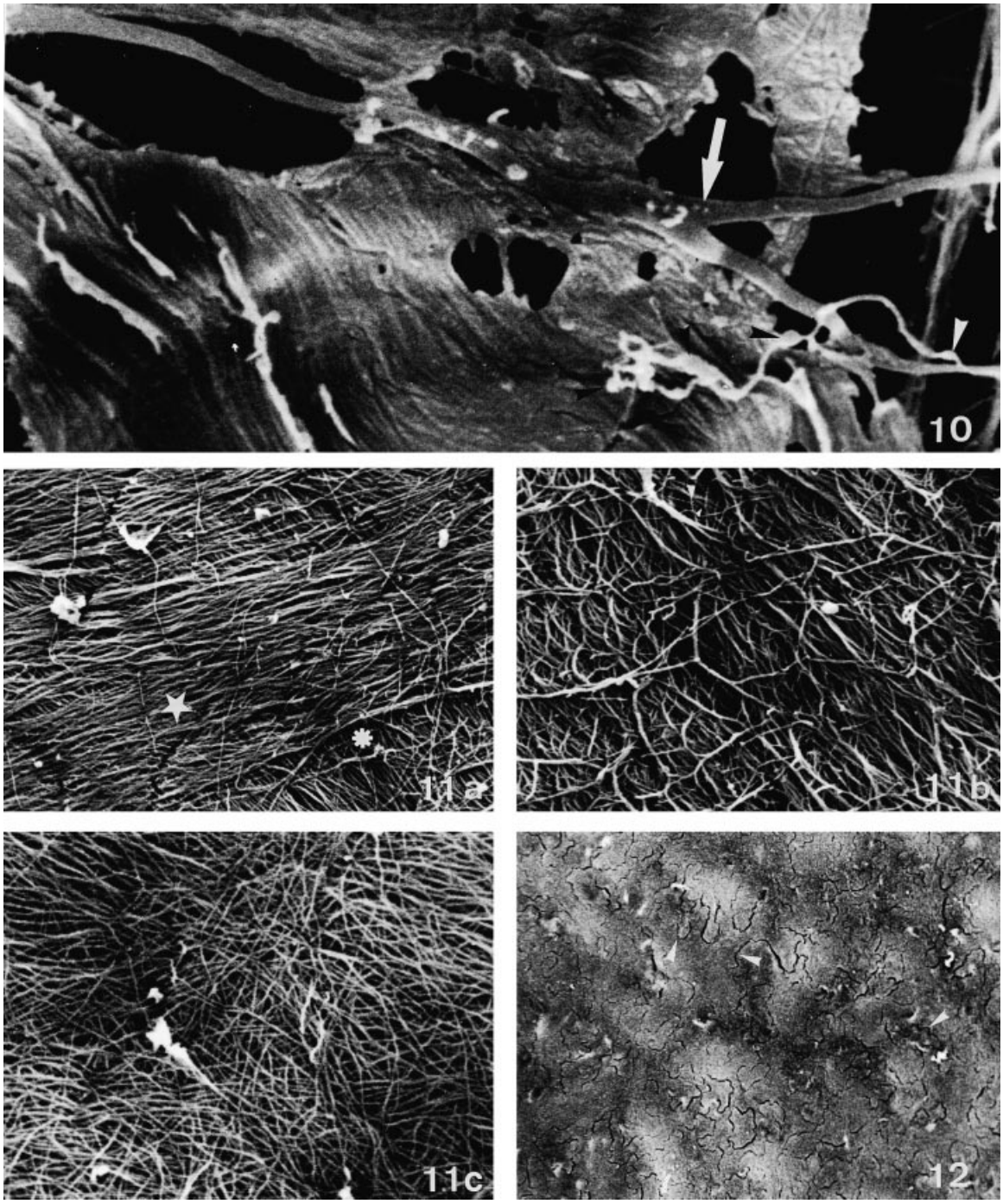

Fig. 10. Micrograph showing the close relationship between axons and keratocytes. Human cornea. HCl digested. Arrowheads, varicosities in a axon; Arrow, stromal neural plexus. $\times 7000$.

Fig. 11. Posterior views of banded portion of Descemet's membrane in the rabbit (*a*, *b*) and human (*c*) cornea. (*a*, *c*) Central cornea; (*b*) peripheral cornea. Asterisk, anterior layer; star, posterior layer. NaOH digestion. $\times 5500$.

Fig. 12. Basal view of the corneal endothelium showing the lateral cell interdigitations (arrowheads). Human cornea. HCl digestion. $\times 3000$.

of different diameters (Figs 8*c–f*, 9*a*), the stromal neural plexus. This plexus appeared apposed to the keratocyte layers. The axons often exhibited varicosities (Figs 9*b*, 10) and ran in close contact with the keratocyte bodies, appearing to be fitted into a shallow depression on the keratocyte surface (Figs 9*b*, 10). Several axons could be seen to establish contact with the same keratocyte (Fig. 9*b*). Axon density appeared to be higher in the rabbit (Fig. 8*d*) than in the human cornea (Fig. 8*e*). No differences in axon density between the anterior and posterior parts of the stroma were observed in rabbits or in humans.

Descemet's membrane

NaOH-digestion eliminated the non-banded portion of Descemet's membrane, allowing us to observe its banded portion.

In the rabbit cornea, the 3D arrangement of the banded portion of Descemet's membrane varied according to the corneal area studied. In the central cornea, this membrane, as viewed from its endothelial surface (non-banded zone), consisted of 2 layers of collagen fibrils (Fig. 11*a*). The posterior layer was discontinuous and was formed by parallel bundles of fibres, whereas the anterior layer was a continuous plate of parallel fibres. The fibres of the 2 layers crossed each other at an angle of about 110°. In the peripheral cornea, close to the sclerocorneal angle, the collagen fibres of Descemet's membrane were arranged in reticular fashion (Fig. 11*b*).

In contrast, in the human cornea, the banded portion of Descemet's membrane exhibited in all areas a thin layer of fibres crossing each other in without a definite pattern (Fig. 11*c*).

Endothelium

In both the rabbit and the human cornea, the endothelial basal surface exhibited tortuous interdigitations between neighbouring cells (Fig. 12).

DISCUSSION

Our SEM observations provide new data on the microanatomy of all layers of the rabbit and human cornea, and also reveal a number of differences between the corneas of these 2 species.

Epithelium

It has been suggested that one function of the microplicae present in the more superficial epithelial cells of the cornea may be to assist in holding the tear film. The tear film forms an air-liquid interface that constitutes the main refractive surface of the mammalian eye. The presence of microplicae in cells of fish corneas (Harding et al. 1974) has raised doubts about the tear film-holding role of the microplicae. The presence, in our observations, of microplicae in epithelial cells not in contact with the tear film seems to support the idea (Lemp et al. 1970) that they could have other functions, such as facilitating the transport of molecules by increasing cell surface.

Transmission electron microscopy has revealed the presence of a complex system of extracellular fibres and surface specialisations which serves to attach the corneal epithelium to the Bowman layer (Marshall et al. 1993). The methods used here do not allow us to repeat those observations.

The present results indicate that the 3D organisation of the human and rabbit EBM is similar to that observed with SEM in other basement membranes (Sawada, 1981; Allen et al. 1988). Our observations also reveal that the human and rabbit EBM are formed of a thin layer of fibres. The differences in the 3D organisation of the EBM between rabbits and humans have not previously been described. These differences could be due to the close relationship between the EBM and the Bowman layer in humans, whereas the rabbit cornea lacks this layer (Kaye & Pappas, 1962). The presence of cross-striated fibres should correspond to the collagenous component of the lamina fibroreticularis. Curiously, our morphological observations on the human EBM are very similar to previous observations reported to pertain to the Bowman layer (see Figure 6 from Komai & Ushiki, 1991). We believe that this is a misinterpretation. The Bowman layer can be clearly differentiated from the EBM by the adhesive tape method (Fig. 3*c*)

The access of nerve fibres to the epithelium is a controversial topic in corneal innervation. It is not yet clear whether epithelial innervation is derived from the limbal neural plexus (Lim & Ruskell, 1978) or from both the limbal neural plexus and stromal neural plexus (Matsuda, 1968; Schimmelpfennig, 1982). In the first case, the nerve fibres reach the epithelium directly, whereas in the second, the stromal nerve fibres would penetrate both the Bowman layer and the EBM to gain access to the epithelium. This study provides evidence that the EBM of both the rabbit and human cornea is perforated by the stromal nerve fibres, results which are consistent with the observations of Müller et al. (1996) and of Komai & Ushiki (1991) for the human cornea.

Stroma

The 3D lamellar organisation has been studied with SEM by means of cryofracture in the rabbit cornea (Cintron et al. 1982) and by NaOH digestion in the human cornea (Komai & Ushiki, 1991). We have observed that the lamellae frequently branch, as suggested by Polack's (1961) findings with silver stains. In addition, the lamellae are not simply

superposed but intertwined (Komai & Ushiki, 1991). This finding is important for corneal biomechanics, since this arrangement could provide the cornea with high tensile strength (Maurice & Monroe, 1990), and for corneal transparency. Our observation of the high variability of the angles formed by two contiguous lamellae is consistent with light microscopic studies (Polack, 1961; Maurice, 1984). No clear differences in lamellar microanatomy between the rabbit and the human cornea were found in the present study.

Keratocyte morphology has only been studied with a methodology similar to ours in the rat cornea (Nishida et al. 1988). We used HCl digestion to remove stromal extracellular materials and this method, as occurs with other organs (Ojeda, 1997), results in good preservation of the keratocyte surface structures. In the current SEM study, we demonstrated for the first time the presence of linear depressions in the keratocyte surface. They may simply be the imprint left by the collagen fibres on the keratocyte surface or they may represent extracellular compartments that allow proper assembly of the collagen fibres. Matrix deposition requires active cellular participation to produce a matrix with the proper size, shape, location and orientation, and it is with this purpose that the fibroblasts, in general, compartmentalise the extracellular space (Birk & Trelstad, 1984; Birk et al. 1991).

One remarkable observation in this study is the presence of fenestrations in the keratocytes. Large and medium-sized fenestrations are present in the keratocytes of both rabbit and human corneas, but the small fenestrations grouped in fields were only observed in the human PSK. This type of fenestration was first demonstrated by Müller et al. (1995). The present finding of a greater number of fenestrations in the PSK than in the ASK in the 2 types of cornea studied seems to support the notion that the fenestrations represent pathways for free nutrients and metabolite diffusion, as proposed by Müller et al. (1995). Since the traffic of molecules through the cornea is accomplished fundamentally in the endothelium-epithelium direction (Klyce & Beuerman, 1988), the presence of numerous fenestrations would facilitate diffusion by enabling molecules to overcome the obstacle presented by superposed layers of keratocytes.

The current data provide unsurpassed images of the 3D organisation and interconnectivity of the keratocyte network. In addition to the horizontal communication between keratocytes (Watsy, 1995; Poole et al. 1996), our observations show interconnectivity between keratocytes located in contiguous layers by means of cellular bridges. This provides the morphological basis of the antero-posterior communication between keratocytes, and is consistent with the dye-injection study of Watsky (1995).

Nerve fibres invaginating keratocytes have previously been described in light (Tervo, 1977) and transmission electron microscopy (Müller et al. 1996) studies, but had not been observed with SEM. Our observations reveal that the keratocytes are frequently in contact with 2 or more nerve fibres. This suggests that the keratocytes are directly innervated. The implications of these observations are not fully understood. It is possible that the nerve fibres modulate the cohesive responsiveness of keratocytes.

Our SEM observations also reveal that the stromal neural plexus is richer in rabbits than in human. The significance of this finding is uncertain. Axon density also appears to be different in the rat (Jacot et al. 1997). However, direct comparison between the 2 studies is difficult due to the different methods used. The presence of nerve fibres with varicosities is consistent with previous transmission electron microscope observations (Matsuda, 1968).

The existence of several types of keratocyte has been reported for lectin-staining (Schanzlin et al. 1990), confocal laser (Poole et al. 1996) and transmission electron microscopy (Müller et al. 1995), in the cornea of different mammalians including humans and rabbits. The 2 keratocyte types observed in the present study do not coincide with those previously described, which may be due to the different methods used. The functional significance of the different keratocytes remains unknown.

Our observation of a greater ASK than PSK density agrees with the results of Møller-Pederson & Ehlers (1995).

Descemet's membrane

Descemet's membrane is the thick basement membrane of the corneal endothelium. It is composed of an anterior banded portion, very rich in collagen, and a posterior non-banded portion, which shows a homogeneous granular appearance (Beurman & Pedroza, 1996). Short attachment fibres are found perpendicular to the interface between the stroma and the Descemet's membrane (Binder et al. 1990).

NaOH digestion eliminates the non-banded portion of the Descemet's membrane, leaving in place the banded, collagenous portion. This portion exhibits a uniform 3D organisation in humans, and has been apparently mistaken with the posterior side of the

stroma in a previous study (Komai & Ushiki, 1991). Structural differences between the human and rabbit Descemet's membrane may be attributable to the different biomechanical requirements of the 2 corneas.

Endothelium

The tortuous interdigitations presented by the endothelial lateral cell membranes in the 2 types of cornea studied considerably increase their lateral surface area, and may be related to the active metabolic pump function of these cells (Green, 1991).

In conclusion, in addition to the lack of a Bowman layer in the rabbit cornea, the main differences in the 3D microanatomy between the human and rabbit cornea lie in the arrangement of the basement membrane collagen fibres, the presence of small fenestrations in the human PSK, the density of the stromal neural plexus, and the arrangement of the collagen fibres in Descemet's membrane.

ACKNOWLEDGEMENTS

The authors are indebted to Ian A. Williams for revising the English manuscript. This work was supported by a grant (PB98-1418-C02-02) from Dirección General de Enseñanza Superior e Investigación.

REFERENCES

ALLEN TD, APLIN JD, CAMPBELL S (1988) Surface visualisation of tissue interfaces by scanning electron microscopy. Methods for exposure of the basal lamina and associated structures in human amnion. *Scanning Microscopy* **2**, 2067–2076.

BEUERMAN RW, PEDROZA L (1996) Ultrastructure of human cornea. *Microscopy Research and Technique* **33**, 320–335.

BINDER PS, ROCK ME, SCHMIDT KC, ANDERSON JA (1991) High-voltage electron microscopy of normal human cornea. *Investigative Ophthalmology & Visual Science* **32**, 2234–2243.

BIRK DE, TRELSTAD RL (1984) Extracellular compartments in matrix morphogenesis: collagen fibril, bundle and lamellar formation by corneal fibroblasts. *Journal Cell Biology* **99**, 2024–2033.

BIRK DE, SILVER FH, TRELSTAD RL (1991) Matrix assembly. In *Cell Biology of Extracellular Matrix* (ed. Hay ED), pp. 221–254. New York: Plenum Press.

CINTRON C, SZAMIER RB, KUBLIN CL (1982) Scanning electron microscopy of the rabbit corneal scars. *Investigative Ophthalmology & Visual Science* **23**, 50–63.

DE RUITER MC, POELMANN RE, MENTINK MMT, VANIPER L, GITTERBERG-DE GROOT AC (1993) Early formation of the vascular system in quail embryos. *Anatomical Record* **235**, 261–274.

DOUGHTY MJ (1990) On the evaluation of the corneal epithelial surface by scanning electron microscopy. *Optometry and Vision Sciences* **67**, 735–756.

EVAN AP, DAIL WG, DAMMROSE D, PALMER C (1976) Scanning electron microscopy of cell surfaces following removal of extracellular material. *Anatomical Record* **185**, 433–446.

GREEN K (1991) Corneal endothelial structure and function under normal and toxic conditions. *Cell Biology Review* **25**, 169–207.

HARDING CV, BAGCHI M, WEINSIEDER A, PETERS VA (1974) Comparative study of corneal epithelial cell surfaces utilizing the scanning electron microscope. *Investigative Ophthalmology* **13**, 906–912.

JACOT JL, GLOVER JP, ROBINSON WG (1997) Computer analysis of corneal innervation density using a novel double stain in rat corneal whole mounts. *Journal of Anatomy* **191**, 191–199.

KAYE GI, PAPPAS GD (1962) Studies on the cornea. I. Fine structure of the rabbit cornea and the uptake and transport of colloidal particles by the cornea in vivo. *Journal Cell Biology* **12**, 457–479.

KLYCE SD, BEUERMAN RW (1988) Structure and function of the cornea. In *The Cornea: Structure and Function of the Cornea* (ed. Kaufman HE, Barron BA, McDonald MB, Waltman SR), pp. 3–54. New York: Churchill Livingstone.

KOMAI Y, USHIKI T (1991) The three-dimensional organization of collagen fibrils in the human cornea and sclera. *Investigative Ophthalmology & Visual Sciences* **32**, 2244–2258.

LEMP MA, HOLLY FJ, IWATA S, DOHLMAN CH (1970) The precorneal tear film. I. Factors in spreading and maintaining a continuous tear film over the corneal surface. *Archives of Ophthalmology* **83**, 89–94.

LIM CH, RUSKELL GL (1978) Corneal nerves access in monkeys. *Graefe's Archives of Clinical and Experimental Ophthalmology* **208**, 15–23.

MARSHALL GE, KONSTAS AG, LEE WR (1993) Collagens in ocular tissues. *British Journal of Ophthalmology* **77**, 515–524.

MATSUDA H (1968) Electron microscopic study on the corneal nerve with special reference to nerve endings. *Japan Journal of Ophthalmology* **12**, 163–173.

MAURICE DM (1984) The cornea and sclera. In *The eye. Vol. 1B: Vegetative Physiology and Biochemistry* (ed. Davson H), pp. 1–58. New York: Academic Press.

MAURICE DM, MONROE F (1990) Cohesive strength of corneal lamellae. *Experimental Eye Research* **50**, 59–63.

MØLLER-PEDERSEN T, EHLERS NA (1995) Three-dimensional study of the human corneal keratocyte density. *Current Eye Research* **14**, 459–464.

MÜLLER LJ, PELS L, VRESEN GJM (1995) Novel aspect of the ultrastructural organization of human corneal keratocytes. *Investigative Ophthalmology & Visual Science* **36**, 2557–2567.

MÜLLER LJ, PELS L, VRESEN GJM (1996) Ultrastructural organization of human corneal nerves. *Investigative Ophthalmology & Visual Science* **37**, 476–488.

NISHIDA T, YASUMOTO K, OTORI T, DESAKI J (1988) The network structure of corneal fibroblasts in the rat as revealed by scanning electron microscopy. *Investigative Ophthalmology & Visual Science* **29**, 1887–1890.

OHTANI O (1987) Three dimensional organization of the connective tissue fibers of human pancreas. A scanning electron microscopy study of NaOH treated tissue. *Archivum Histologicum Japonicum* **50**, 557–566.

OJEDA JL (1997) *Métodos de Microscopia Electrónica de Barrido*, pp. 81–117. Santander: Universidad de Cantabria.

POOLE CA, BROOKES NH, CLOVER GM (1996) Confocal imaging of the keratocyte network in porcine cornea using the fixable vital dye 5-chloromethylfluorescein diacetate. *Current Eye Research* **15**, 165–174.

POLACK FM (1961) Morphology of the cornea. I. Study with silver stains. *American Journal of ophthalmology* **51**, 1051–1056.

SAWADA H (1981) Structural variety of basement membranes: a scanning electron microscopy study. *Biomedical Research* **2**, 125–128.

SCHANZLIN DJ, KRATZ-OWENS K, HAGEMAN GS (1990) Keratocyte subpopulation as revealed by lectin-binding. *Investigative Ophthalmology & Visual Science* **31**, 32–33.

SCHIMMELPFENNIG B (1982) Nerve structures in human central cornea epithelium. *Graefe's Archives of Clinical and Experimental Ophthalmology* **218**, 14–20.

TERVO T (1977) Consecutive demonstration of nerves containing catecholamine and acetylcholinesterase in the rat cornea. *Histochemistry* **50**, 291–299.

WATSKY MA (1995) Keratocyte gap junctional communication in normal and wounded rabbit corneas and human corneas. *Investigative Ophthalmology & Visual Science* **36**, 2568–2576.